

**Synthesis, Structure, Properties, and Cytotoxicity of a
(Quinoline)RuCp⁺ Complex**

Journal:	<i>Dalton Transactions</i>
Manuscript ID	DT-ART-10-2022-003484.R1
Article Type:	Paper
Date Submitted by the Author:	28-Nov-2022
Complete List of Authors:	Hou, Zhilin; Michigan State University, Chemistry Vanecek, Allison; Michigan State University, Chemistry Tepe, Jetze; Michigan State University, Department of Chemistry Odom, Aaron; Michigan State University,

ARTICLE

Synthesis, Structure, Properties, and Cytotoxicity of a (Quinoline)RuCp⁺ Complex

Received 00th January 20xx,
Accepted 00th January 20xx

Zhilin Hou, Allison S. Vanecek, Jetze J. Tepe*, and Aaron L. Odom*

DOI: 10.1039/x0xx00000x

A rare example of a structurally characterized metal quinoline complex was prepared using a non-covalent quinoline-based proteasome inhibitor (**Quin1**) and a quinoline inactive as a proteasome inhibitor (**Quin2**). The quinolines are prepared in a one-pot procedure involving titanium-catalyzed alkyne iminoamination and are bound to ruthenium by reaction with CpRu(NCMe)₃⁺ PF₆⁻ in CH₂Cl₂. The arene of the quinoline is η⁶-bonded to the ruthenium metal center. The kinetics of quinoline displacement were investigated, and reactivity with deuterated solvents goes as acetonitrile > DMSO > water. Quinolines with more methyl groups on the arene are more kinetically stable, and RuCp(Quin1)⁺ PF₆⁻ (**1**), which has two methyl groups on the arene, is stable for days in DMSO. In contrast, a very similar complex (**2**) made with **Quin2** having no methyl groups on the arene was readily displaced by DMSO. Both **1** and **2** are stable in 9:1 water/DMSO for days with no measurable displacement of the quinoline. The cytotoxicity of the quinolines, their CpRu⁺-complexes, and CpRu(DMSO)₃⁺ PF₆⁻ were investigated towards two multiple myeloma cell lines: MC/CAR and RPMI 8226. To determine whether activity of the complexes was related to the nature of the quinoline ligands, two structurally similar quinoline ligands with vastly different biological properties were investigated. **Quin1** is a cytotoxic proteasome inhibitor, whereas **Quin2** is not a proteasome inhibitor and showed no discernable cytotoxicity. The ruthenium complexes showed poor cellular proteasome inhibition. However, both **1** and **2** showed good cytotoxicity towards RPMI 8226 and MC/CAR, with **1** being slightly more cytotoxic. For example, **1** has a CC₅₀ = 2 μM in RPMI 8226, and **2** has a CC₅₀ = 5 μM for the same cell line. In contrast CpRu(DMSO)₃⁺ PF₆⁻ was quite active towards MC/CAR with CC₅₀ = 2.8 μM but showed no discernable cytotoxicity toward RPMI 8226. The mechanism of action responsible for the observed cytotoxicity is not known, but the new Ru(Cp)(Quin)⁺ PF₆⁻ complexes do not cross-link DNA as found for platinum-based drugs. It is concluded that the Ru(Cp)(Quin)⁺ PF₆⁻ complexes remain intact in the cellular assays and constitute a new class of cytotoxic metal complexes.

Introduction

In the 1960s, fundamental studies into the effect of electric fields on bacterial growth led to the discovery by Barnett Rosenberg and coworkers that some late transition metal complexes, like platinum and ruthenium, will inhibit cell division.¹ They showed that the bacteria were sensitive to platinum complexes derived from their electrodes used in the experiments, which caused no significant reduction in growth rate but did show significant reduction in cell division. The addition of platinum compounds to the growing *E. coli* resulted in filament-like bacteria >300 times the length of a normal cell.² They quickly realized the applications of such compounds to cancer therapy,³ where one great success for these platinum complexes was in testicular cancer. Now, platinum therapeutics like carboplatin, also developed by Rosenberg and coworkers, have a cure rate of >95% for testicular cancer and are used as

part of the “cocktail” for many different types of cancers. As a result, their mechanism of action has been extensively studied.⁴

Even though ruthenium complexes were among those discovered by Rosenberg and coworkers to inhibit cell division,¹ the development of ruthenium complexes into pharmaceuticals has been far slower than their platinum counterparts.⁵ Nevertheless, there is substantial evidence that a variety of different ruthenium complexes display anti-cancer and other biological activity.^{6–8} Notably, in the context of this work, many η⁵-cyclopentadienyl and η⁶-arene complexes have shown promising biological activity.^{5–19}

Many ruthenium complexes are known to have biological activity, and ruthenium(II) forms many stable cationic arene complexes.^{20–23} We decided to use a CpRu⁺ fragment for this study as it is readily accessible, forms stable arene complexes, and has derivatives that are known to inhibit cancer cell proliferation.^{24–26} Surprisingly, the only η⁶-quinoline complex with any transition metal center in the CCDC database as of this writing (CSD version 5.43, Nov 2021) is (quinoline)Mo(PMe₃)₃ by Parkin and coworkers (Chart 1).²⁷ However, there are a few ruthenium-quinoline complexes that have been reported, and some are shown in Chart 1. Fish and coworkers reported the synthesis of CpRu(quinoline)⁺ (and Cp*) from CpRu(pyridine)(NCMe)₂⁺ in 1989 and described haptotropic

^a Michigan State University, Department of Chemistry, 578 S. Shaw Ln, East Lansing, MI 48824. odoma@msu.edu, tepe@msu.edu

Electronic Supplementary Information (ESI) available: Additional experimental details and data. NMR spectra for new compounds. Dose-response curves for the proteasome inhibition and cytotoxicity studies. The single crystal X-ray diffraction data has been submitted to the Cambridge Structural Database and assigned reference number 2153369. See DOI: 10.1039/x0xx00000x

ARTICLE

Journal Name

shifts of the heterocycles.²⁸⁻³⁰ More recently, Holman and Fairchild used $(\text{RuCp}^*\text{Cl})_4$ with quinoline to produce $\{(\text{quinoline})\text{RuCp}^*\}^+ \text{Cl}^-$.^{31, 32}

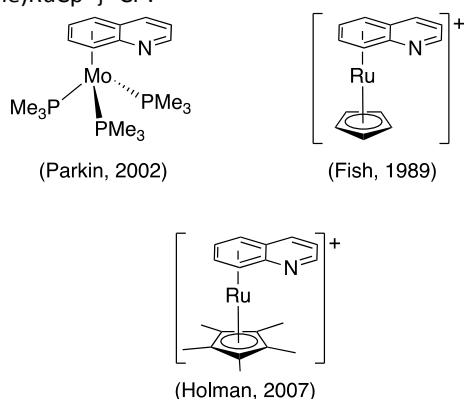


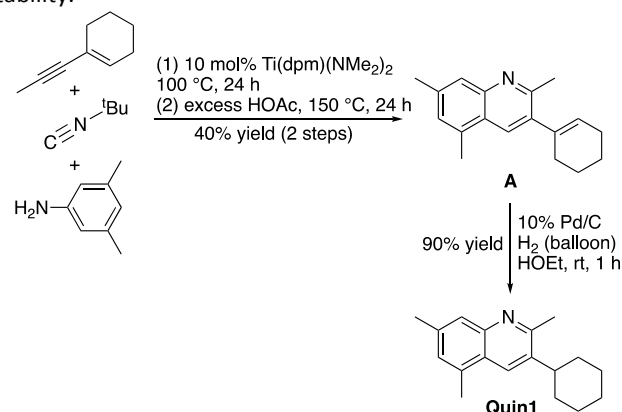
Chart 1. Parkin and coworkers structurally characterized example of an η^6 -quinoline complex, $(\text{quinoline})\text{Mo}(\text{PMe}_3)_3$,²⁷ along with some examples of ruthenium quinoline complexes from the literature that do not have structures in the CCDC database but are likely η^6 -coordinated.

Cyclopentadienyl ruthenium complexes have been investigated for their anti-cancer activity, with their cytotoxicity mechanism dependent upon the co-ligands on the metal center, which are highly varied. As examples, cytotoxicity of CpRu complexes has been ascribed to GSK3beta and PI3K inhibition, PARP-1 inhibition, and cell death induced through the Golgi apparatus.^{5, 33-45} Various CpRu complexes have shown some activity against a variety of cell types including HL-60 (human leukemia), LoVo (human colon adenocarcinoma), MiaPaCa (pancreatic cancer), A2780 (cisplatin resistant human ovarian), MCF7 (human breast), PC3 (human prostate), MM96L (human skin carcinoma), MDA-MB-231 (hormone-independent breast cancer), and HeLa (cervical carcinoma).^{5, 33-45} In some cases, Ru complexes were found to be many times more active than cisplatin. Among the ruthenium complexes, CpRu(arene)⁺ systems have been investigated against several different cell lines as well.^{5, 33-45}

In previous work, our research groups have published quinoline-core compounds with significant promise as proteasome inhibitors.⁴⁶ Modulation of proteasome activity has become an important method for the treatment of several diseases, including certain cancer types such as multiple myeloma.^{47, 48} For multiple myeloma, competitive inhibitors like bortezomib are included in the treatment, but the pharmacodynamic properties of these compounds restrict their use to blood-based cancers. Noncovalent inhibitors, such as the quinoline-based inhibitors being studied here, could lead to broader clinical applications.^{46, 49-52}

Of particular interest in this study is a specific quinoline-based proteasome inhibitor with a cyclohexyl group on the 3-position (Scheme 1), **Quin1**.⁴⁶ The precursor to **Quin1**, **A**, was prepared using a one-pot procedure involving titanium-catalyzed multicomponent coupling (alkyne iminoamination) followed by acetic acid-catalyzed cyclization (Scheme 1).^{53, 54} The vinyl group on the alkyne leads to excellent regioselectivity for the quinoline product **A** shown. The vinyl group is then reduced in

high yield by Pd/C and H₂ to give a compound with good proteasome inhibition activity and excellent microsomal stability.⁴⁶



Scheme 1. Synthesis of quinoline-based proteasome inhibitor, **Quin1**.

Multi-targeted therapeutics are of great potential utility in cancer treatments, and ruthenium systems have been looked at in some detail, including η^6 -aromatics ruthenium complexes.¹³ For example, the ruthenium may be incorporated with another compound coordinated datively that acts on a different cellular system, e.g., a kinase or P450 inhibitor.⁵⁵ Combinations of drugs are almost invariably employed in cancer treatment, and proteasome inhibitors have been investigated in combination with cisplatin to great effect,⁵⁶ and these drug combinations can show synergistic effects.⁵⁷ Here, we discuss the synthesis, properties, and biological activity of η^6 -quinoline ruthenium complexes, such as sandwich complex CpRu(Quin1)⁺ PF₆⁻ (**1**), their stability in vitro and in cell culture, and their cytotoxicity towards two multiple myeloma cell lines. As part of these investigations, we hoped to determine if the complex fragments to CpRuL₃⁺ PF₆⁻ and a quinoline species, which act in tandem for cell cytotoxicity, or if the ruthenium quinoline complex remains intact within the cell. To accomplish this, the bio-active ligand **Quin1** was used in conjunction with a closely related inactive quinoline ligand, **Quin2**, as ligands for ruthenium. This allowed us to determine that (vide infra) the quinolines were not lost in the cells as indicated by a lack of proteasome inhibition and that quinoline ruthenium complexes themselves are cytotoxic agents.

Results and Discussion

The synthesis of Ru(Cp)(Quin1)⁺ PF₆⁻ (**1**) was possible from CpRu(NCMe₃)₃⁺ PF₆⁻ by simple addition of **Quin1** in dichloromethane at room temperature. The recrystallized product was available in 50% yield. Single crystals for X-ray diffraction were obtained by layering a CH₂Cl₂ solution of **1** with OEt₂ and cooling to -35 °C.

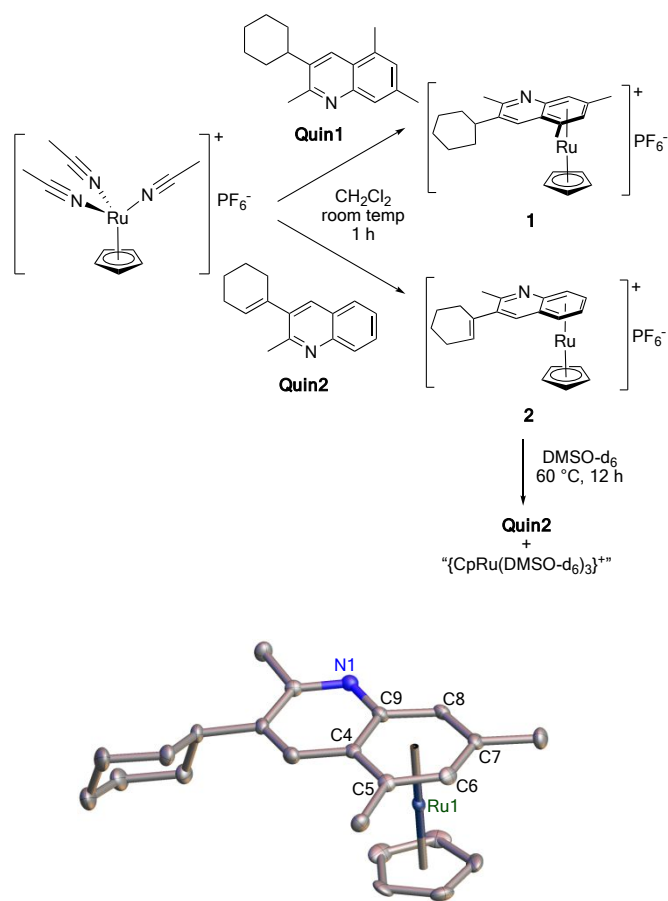
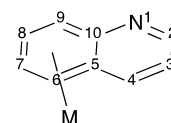


Fig. 1. Synthesis and structure of Ru(Quin1)(Cp)⁺ PF₆⁻ (**1**). The PF₆⁻, a molecule of CH₂Cl₂ from crystallization, and hydrogens are not shown in the ORTEP diagram from the single-crystal X-ray diffraction experiment of **1**.

Complex **1** exhibits a typical sandwich structure with a centroid-Ru-centroid angle of 177.33(3)°. The five carbons of the cyclopentadienyl ligand are nearly equidistant from the ruthenium center, varying from 2.195(4) to 2.169(4) Å. In contrast, the Ru–C distances to the η⁶-aromatic vary somewhat with substituents. The two carbons involved in the fusion to the nitrogen-containing ring (C4 and C9) are the farthest from the metal center at 2.256(3) and 2.278(4) Å, respectively, with the carbon connected to the electron-withdrawing nitrogen perhaps slightly farther from the metal. It is the carbons with methyl groups, especially C7, that are slightly longer from the metal center than the unsubstituted carbons of the aromatic, but the values are within 3 estimated standard deviations. Overall, the quinoline ring leans slightly away from the carbons involved in the fusion to the nitrogen ring, but not significantly.

Comparing the structure of **1** and (quinoline)Mo(PMe₃)₃ with the structure of free quinoline,⁵⁸ one can see how metal coordination affects the C–C distances within the rings (Table 1). Consistently, the bond distances in the coordinated aromatic ring are either unaffected by coordination or slightly lengthened. Only a few distances are lengthened significantly (beyond 3 e.s.d.) in both structures: 5-6, 6-7, and 8-9.

Table 1. Comparison of C–C bond distances (Å) in uncoordinated quinoline (quin) and in η⁶(C₆)-complexes Ru(Quin1)Cp⁺ PF₆⁻ (**1**) and (quinoline)Mo(PMe₃)₃.



Bond Position	quin ⁵⁸	1	1 – quin ^a	(η ⁶ (C ₆)-quin)Mo(PMe ₃) ₃	Mo(quin) – quin ^a
1-2	1.320(2)	1.311(5)	-0.009	1.310(6)	-0.01
2-3	1.406(2)	1.461(5)	0.055	1.388(5)	-0.018
3-4	1.359(2)	1.360(5)	0.001	1.350(6)	-0.009
4-5	1.411(2)	1.432(5)	0.021	1.412(6)	0.001
5-10	1.418(2)	1.441(5)	0.023	1.433(6)	0.015
5-6	1.410(2)	1.440(5)	0.030	1.435(6)	0.025
6-7	1.360(2)	1.417(5)	0.057	1.398(7)	0.038
7-8	1.405(2)	1.423(5)	0.018	1.392(7)	-0.013
8-9	1.358(2)	1.420(5)	0.062	1.421(7)	0.063
9-10	1.417(2)	1.425(5)	0.008	1.422(6)	0.005
1-10	1.367(2)	1.383(5)	0.016	1.381(5)	0.014

^aDifferences in the distances between coordinated and uncoordinated quinolines outside of three standard deviations are shown in red.

During our investigations into the properties of **1**, it was discovered that the complex is unstable in the presence of acetonitrile. This phenomenon with respect to (η⁶-arene)Ru(II) complexes has been noted before; Fish and coworkers reported that {(η⁶-2-Me-quinoline)Ru(Cp)}⁺ in the presence of excess MeCN provides the free quinoline and {Ru(Cp)(NCMe)₃}⁺ after 2 days at ambient temperature.²⁹ The kinetics of hydrocarbon η⁶-arene displacement were studied in detail by McNair and Mann, who established a second-order rate law, $rate = k_{obs} [Complex][CH_3CN]$, for arene displacement.⁵⁹

The reaction of **1** with acetonitrile-d₃ as solvent requires a couple of days at room temperature (Fig. 2). Fitting⁶⁰ either the loss of η⁶-quinoline starting material or production of Ru(Cp)(NCCD₃)₃⁺ PF₆⁻ product gives similar rate constants, and the average pseudo-first order rate constant was $k_{obs} = (7.0 \pm 1.9) \times 10^{-6} \text{ s}^{-1}$ at the 95% confidence interval,⁶¹ which was found by averaging the rate constants for product formation and starting material loss over 3 separate runs, i.e., 6 total values. The observed rate constant for quinoline loss in **1** is somewhat smaller than that reported for loss of quinoline in Ru(η⁶-quinoline)(Cp)⁺ PF₆⁻ of $4.1 \times 10^{-5} \text{ s}^{-1}$, also under pseudo-first order conditions.⁵⁹

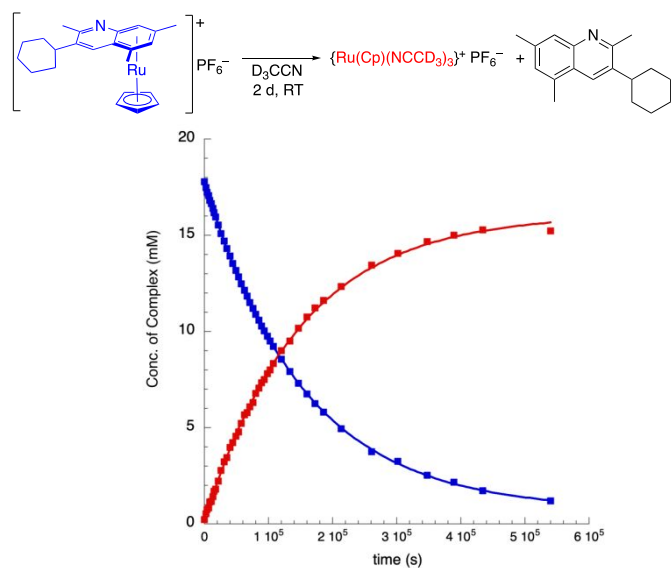


Fig. 2. Reaction of Ru(Quin1)Cp⁺ PF₆⁻ (**1**) with acetonitrile-*d*₃ leads to release of the quinoline and formation of Ru(Cp)(NCCD₃)₃⁺ PF₆⁻. The concentration vs. time data are fit to $Y_t = Y_\infty + (Y_0 - Y_\infty)e^{-k_{obs}t}$, where Y_t = conc. at time t , Y_0 = conc. at the start of the reaction, Y_∞ = conc. at very long times, and k_{obs} is the observed pseudo-first order rate constant in s⁻¹. For growth of product (red): $Y_\infty = 16.08 \pm 0.08$, $Y_0 = 0.15 \pm 0.4$, $k_{obs} = (6.72 \pm 0.08) \times 10^{-6}$, $R^2 = 0.9994$. For loss of **1** (blue): $Y_\infty = 0.70 \pm 0.03$, $Y_0 = 17.8 \pm 0.1$, $k_{obs} = (6.45 \pm 0.02) \times 10^{-6}$, $R^2 = 0.99997$.

Interestingly, Ru(Quin1)Cp⁺ PF₆⁻ (**1**) is stable in other coordinating solvents. For example, **1** was dissolved in DMSO-*d*₆ and 1:9 DMSO-*d*₆/D₂O. NMR experiments involving **1** in these solvents show no reaction at room temperature over the course of 72 h.

To investigate further, and for testing of biological activity, we prepared a slightly modified version of **1** (Fig. 1). A quinoline that only differs from **Quin1** in that it doesn't have the methyl groups on the aromatic ring was prepared, **Quin2**. The biological activity of **Quin1** and **Quin2** are quite different in proteasome inhibition assays (vide infra),⁴⁶ but the two quinolines also behave differently as ligands for ruthenium. The η⁶-quinoline complex Ru(Quin2)Cp⁺ PF₆⁻ (**2**) was prepared using a similar procedure to **1**. However, dissolving **2** in DMSO-*d*₆ or MeCN-*d*₃ results in rapid appearance of free quinoline in the ¹H NMR spectrum. In other words, removal of the methyl groups on the aromatic ring results in a metal complex where the quinoline is more readily displaced by solvents. The reaction of **2** with DMSO-*d*₆ gives free **Quin2** and a new RuCp complex, CpRu(DMSO-*d*₆)₃⁺ PF₆⁻, over the course of a few hours. However, in 1:9 DMSO-*d*₆:D₂O, complex **2** appears to be stable for days.

The thermodynamics of hydrocarbon π-systems binding to related Cp*Ru(NCMe)₃⁺ have been investigated in some detail by Nolan and coworkers.⁶² Naphthalene, the closest hydrocarbon to quinoline, reacts with Cp*Ru(NCMe)₃⁺ in THF to give {Cp*Ru(naphthalene)}⁺, but the reaction is exothermic by only a small margin, ΔH_{rxn} = -1.7 ± 0.1 kcal/mol. Benzene coordination to the same fragment is about twice as exothermic. Addition of electron-donating groups (e.g., Me,

SiMe₃, OMe, and NMe₂) thermodynamically stabilizes the η⁶-arene complex significantly. In addition to this thermodynamic issue with quinoline binding, kinetic replacement of naphthalene over benzene is favored due to the “naphthalene effect”,⁶³ similar to the more familiar “indenyl ligand effect” identified by Basolo and coworkers where rearomatization of a coordinated fused ring system leads to lower barriers for ring slipping and faster ligand substitution.^{64, 65}

Biological Activity of η⁶-Quinoline Ruthenium Complexes

The ubiquitin-proteasome system (UPS) is one of the two degradation systems of the proteostasis network responsible for the degradation of damaged, misfolded, and unneeded proteins.⁶⁶ The 20S core particle contains three unique catalytic sites (β5, β2, and β1) responsible for chymotrypsin (CT-L), trypsin (T-L), and caspase-like (Casp-L) proteolytic activity, respectively. The 19S regulatory particle in the UPS functions to recognize ubiquitylated proteins, unfold the target protein, and transfer the unfolded substrate protein into the proteolytic core for degradation.^{67, 68}

Table 2. In vitro 20S proteasome inhibition activities.^a

Compound	CT-L IC ₅₀ (μM)	Casp-L IC ₅₀ (μM)	3 Site IC ₅₀ (μM)
Quin1	9	9	14
Quin2	>80	>80	>80
Ru(Quin1)Cp ⁺ (1)	15	16	30
Ru(Quin2)Cp ⁺ (2)	>80	>80	>80

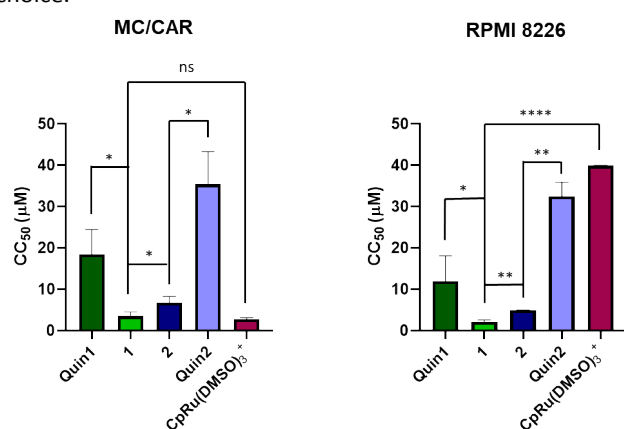
^aThese noncovalent inhibitors are inactive against T-L sites.

We have previously shown **Quin1** to be a low micromolar noncovalent proteasome inhibitor, therefore we sought to explore how the CpRu(quinoline)⁺ complexes would compare. The in vitro proteasome inhibition activity of **Quin1** and **Quin2** along with their respective CpRu⁺ complexes, **1** and **2**, was investigated using fluorogenic peptide substrates.⁴⁶ Consistent with previous results, **Quin1** is inactive for inhibition of T-L sites but is a single-digit micromolar inhibitor of Casp-L and CT-L site proteolytic activity (Table 2). In addition, our negative control **Quin2** is inactive (IC₅₀ > 80 μM) for inhibition of all three catalytic sites of the 20S proteasome. Complexation of **Quin1** to CpRu⁺ to form **1** reduces the proteasome inhibition activity approximately two-fold in vitro. The addition of **Quin2** to CpRu⁺ to give **2** does not enhance the quinoline's proteasome inhibition activity, i.e., **2** is also inactive as a proteasome inhibitor.

We investigated the activity of the quinoline and ruthenium complexes as cytotoxic agents against two different cell lines of multiple myeloma origins: MC/CAR and RPMI 8226. The results are shown graphically and tabulated in Fig. 3. The results are generally similar for each of the two distinct cell lines. As expected, the inactive quinoline (**Quin2**) did not show appreciable cytotoxicity. The active proteasome inhibitor **Quin1** was moderately cytotoxic with CC₅₀ values consistent with its IC₅₀ values found in the in vitro proteasome activity assays. Both

ruthenium complexes **1** and **2** were significantly more cytotoxic than either of the quinoline counterparts, indicating that the cytotoxicity is not related to the activity of disassociated quinoline.

To determine if this enhanced cytotoxicity upon complexation was due to the dissociated CpRu⁺ species, a ruthenium control using DMSO as ligands, CpRu(DMSO)₃⁺ PF₆⁻, was tested for cytotoxicity in both cell lines. While CpRu(DMSO)₃⁺ PF₆⁻ was not cytotoxic in RPMI 8226 cells at the concentrations tested, its cytotoxicity in MC/CAR cells was comparable to both complexes **1** and **2**. This suggests sensitivity to CpRu(DMSO)₃⁺ PF₆⁻ toxicity is cell line specific. In the MC/CAR cell line, all ruthenium complexes had similar cytotoxicity curves with comparable single digit micromolar CC₅₀ values; however, in the RPMI 8226 cell line, ruthenium toxicity was observed to enhance greatly upon addition of the quinoline ligands. This result was expected as ruthenium cytotoxicity is tunable based on the ligand of choice.



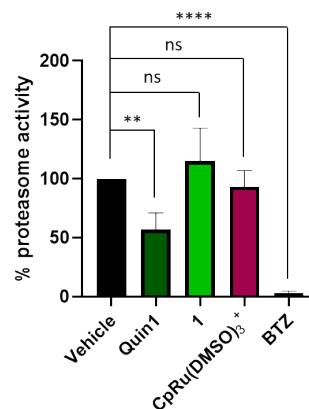
Compound	MC/CAR CC ₅₀ (μM)	RPMI 8226 CC ₅₀ (μM)
Quin1	19.5	11.8
Quin2	>40.0	32.4
CpRu(DMSO) ₃ ⁺	2.8	>40.0
Ru(Quin1)Cp ⁺ (1)	3.4	2.0
Ru(Quin2)Cp ⁺ (2)	6.8	5.0
Bortezomib (BTZ)	<1.3	<1.3

Fig. 3. Cytotoxicity data for MC/CAR and RPMI 8226 (n = 4). Brown-Forsythe and Welch ANOVA with a post hoc Dunnett's T3 test was used for multiple comparisons of group means. (* p ≤ 0.05, ** p ≤ 0.01)

Further studies to explore the mechanism of cytotoxicity in the RPMI 8226 cell line were conducted. While ruthenium complexes **1** and **2** were significantly more cytotoxic than either of the free quinoline counterparts, a minimal difference in cytotoxicity was observed upon incorporation of the active or inactive quinoline, suggesting inhibition of the proteasome is likely not the mechanism of cytotoxicity. Additionally, both complexes **1** and **2** were significantly more cytotoxic than either of the quinolines or CpRu(DMSO)₃⁺ PF₆⁻, therefore, we hypothesized that the complexes remain intact in cell culture. As it is expected that the dissociated products of **1** would be a derivative of Ru species (shown to be nontoxic in RPMI 8226) and **Quin1**, it is anticipated that the cytotoxicity of **Quin1** and the dissociated products of **1** would be relatively similar;

however this was not observed. Therefore, we sought to explore whether complexes **1** and **2** remained intact in cell culture to elucidate the mechanism of cytotoxicity of the CpRu quinoline complexes.

The incorporation of the quinoline ligands active or inactive for proteasome inhibition presented a novel approach to explore whether complexes **1** and **2** remained intact in cell culture. Again, since it is expected that the dissociated products of **1** would be RuCp(OH₂)₃⁺ PF₆⁻ and **Quin1**, the cellular proteasome activities of **Quin1** and the dissociated products of **1** should be comparable, as related CpRu(DMSO)₃⁺ PF₆⁻ did not inhibit the proteasome in vitro.



Compound	Percent Proteasome Activity	Percent Cell Viability
Vehicle	100	100
Quin1 (10 μM)	57	97
Ru(Quin1)Cp ⁺ (1) (10 μM)	115	98
CpRu(DMSO) ₃ ⁺ (10 μM)	93	98
Bortezomib (BTZ) (50 nM)	3	81

Fig. 4. Cellular proteasome activity data with corresponding cytotoxicity data in the RPMI 8226 cell line (n = 3). One-way ANOVA with a post hoc Sidak test was used for multiple comparisons of group means. (ns = not significant; ** p ≤ 0.01; **** p ≤ 0.0001)

The cellular proteasome inhibition activities of **Quin1**, complex **1**, and CpRu(DMSO)₃⁺ were investigated in RPMI 8226 cells using a luminescent peptide substrate.⁴⁶ Consistent with the in vitro results, **Quin1** (10 μM) resulted in a 43% reduction in proteasome activity following a 4 h treatment, consistent with the in vitro IC₅₀ value and CC₅₀ value in RPMI 8226 cells (Fig. 4). Complex **1** and CpRu(DMSO)₃⁺ PF₆⁻ did not inhibit the proteasome, ruling out the possibility of proteasome inhibition as the mechanism of cytotoxicity. Furthermore, it suggests complex **1** remains intact in cell culture at this treatment time, as no proteasome inhibition was observed from any liberated **Quin1**. To explore if a longer treatment time would result in decomplexation of **Quin1** from **1**, resulting in proteasome inhibition and cytotoxicity, a lower dose of the test compounds was used to treat the RPMI 8226 cells for 24 h. In this experiment, **Quin 1** (5 μM) resulted in a 36% reduction in proteasome activity (see SI). Treatment with Ru complex **1** (3 μM) did not exhibit proteasome inhibition after correcting for the loss in cell viability. These results provide additional support

that cytotoxicity results from the intact $\text{CpRu}(\text{quinoline})^+ \text{PF}_6^-$ complexes in cell culture.

After eliminating proteasome inhibition as the mechanism of cytotoxicity, we sought to explore possible mechanisms of toxicity by ruthenium. While the mechanism of ruthenium anticancer drugs varies greatly based on the ligands used (vide supra), platinum drugs have been well established to crosslink DNA.⁴ As a first look at mechanism, we explored the ability of complexes **1**, **2**, and $\text{CpRu}(\text{NCMe})_3^+ \text{PF}_6^-$ to crosslink DNA in an in vitro assay using a denaturing gel (see the SI). Compared to the positive control, cisplatin, no DNA crosslinking was observed for the three ruthenium complexes. While no crosslinking was observed, the experiment does not omit the possibility of DNA damage that does not lead to crosslinking as a possible mechanism of cytotoxicity.

Combined, the biological data for the $\text{CpRu}(\text{quinoline})^+ \text{PF}_6^-$ complexes provides strong support that the intact complex is responsible for the cytotoxic effects in cell culture. While the mechanism for cytotoxicity of the quinoline ruthenium complexes is currently unknown, the data suggests the cytotoxicity is based on the ligand incorporated. Use of DMSO as the ligand in the control $\text{CpRu}(\text{DMSO})_3^+ \text{PF}_6^-$ complex did not result in cytotoxicity in RPMI 8226 cells, however, incorporation of either of the quinolines as the ligand greatly enhanced the cytotoxic effects of the complexes. Therefore, it was concluded that the $\text{Ru}(\text{Cp})(\text{Quin})^+ \text{PF}_6^-$ complexes **1** and **2** constitute a new class of cytotoxic metal complexes and provide an intriguing avenue to explore for anticancer therapeutics.

Conclusions

Rare examples of structurally characterized transition metal quinoline complexes were prepared by addition of the free quinoline to $\text{CpRu}(\text{NCMe})_3^+ \text{PF}_6^-$ in CH_2Cl_2 . The metal center binds η^6 to the more electron-rich arene group of the quinoline to give thermodynamically stable species, and the structural parameters are suggestive of significant backbonding to the quinoline ring from the metal center (Table 1) with lengthening of a few C–C bond parameters relative to free quinoline.

The stability of the quinoline-ruthenium interaction is profoundly affected by methylation of the arene ring of the quinoline. In **2**, where there are no methyl groups on the arene ring, the quinoline is readily removed from the metal center by DMSO; in contrast, for **1**, where there are two methyl groups on the arene ring, the complex is stable for days in DMSO. Both **1** and **2** are stable in DMSO/water 1:9 for >3 days. In acetonitrile- d_3 , even more stable **1** loses the arene ring to form **Quin1** and $\text{CpRu}(\text{NCMe})_3^+ \text{PF}_6^-$ with a rate constant of $6 \times 10^{-6} \text{ s}^{-1}$ ($t_{1/2} \sim 30 \text{ h}$). In other words, ruthenium complexes showed different stability in DMSO and MeCN but both seem to be quite stable in aqueous solution.

Here, we investigated whether the η^6 -quinoline ruthenium complexes were stable in cell culture and if they have cytotoxicity towards multiple myeloma cell lines, either through proteasome inhibition or through another mechanism. Known proteasome inhibitors **Quin1** and positive control bortezomib (**BTZ**) showed proteasome inhibition during in vitro and cellular

assays. **Quin2** and the ruthenium complexes **1** and **2** did not show significant proteasome inhibition. Nevertheless, both complexes **1** and **2** show significant cytotoxicity ($\text{CC}_{50} \sim 2\text{--}7 \mu\text{M}$) in both RPMI 8226 and MC/CAR cell lines.

If the **Quin1** ligand in $\text{RuCp}(\text{Quin1})^+ \text{PF}_6^-$ (**1**) were being released in cell culture, one would presume that $\text{RuCp}(\text{OH}_2)_3^+ \text{PF}_6^-$ and **Quin1** would be the products. As a result, proteasome inhibition should have been observed in activity assays for **1**, which was not the case. In addition, while we could not isolate $\text{RuCp}(\text{OH}_2)_3^+ \text{PF}_6^-$, we prepared $\text{RuCp}(\text{DMSO})_3^+ \text{PF}_6^-$ for testing in aqueous solution, and the tris(DMSO) complex showed selective cytotoxicity between the two cell lines, active towards MC/CAR ($\text{CC}_{50} = 2.8 \mu\text{M}$) and inactive towards RPMI ($\text{CC}_{50} > 40 \mu\text{M}$). Since complex **1** shows significant activity towards both multiple myeloma cell lines, the data are inconsistent with quinoline loss from **1**. In conclusion, complex **1** is stable in the cells and shows cytotoxicity through a mechanism of action not related to proteasome inhibition.

In summary, by using a bioactive quinoline ligand and $\text{CpRu}(\text{solv})_3^+$, we were able to show that quinoline is not lost in cell culture. The $\text{Ru}(\text{quinoline})$ complexes do not show significant proteasome inhibition and do not display DNA crosslinking activity using a denaturing gel (see the SI), however, these studies do not rule out the possibility of DNA damage. Consequently, a different, currently unknown, mechanism for cytotoxicity of the $\text{Ru}(\text{quinoline})\text{Cp}^+ \text{PF}_6^-$ complexes must be operative.^{36, 37, 41}

Experimental

General Considerations

All manipulations were carried out under an inert dinitrogen atmosphere in an MBraun glovebox or using standard Schlenk techniques. The solvents toluene, acetonitrile, and diethyl ether were sparged with dinitrogen and passed over an activated alumina column prior to use. *n*-hexane was dried by refluxing with sodium-benzophenone ketyl and distilled under dinitrogen prior to use. Ethanol was dried by refluxing over magnesium and distilled under dinitrogen prior to use. CDCl_3 was purchased from Cambridge Isotope Laboratories, dried over P_2O_5 , and distilled under dinitrogen. All solvents were stored over 3 Å molecular sieves in an inert atmosphere glove box after purification. Synthesis of *tert*-butylisonitrile was done according to the literature procedure and purified by distillation under dry dinitrogen.⁶⁹ Syntheses of $\text{Ti}(\text{dpm})(\text{NMe}_2)_2$ was done according to the literature procedure.⁷⁰ $\text{CpRu}(\text{CH}_3\text{CN})_3^+ \text{PF}_6^-$ was prepared by a modification of the literature procedure, and the details of the modifications can be found in the SI.⁷¹ **Quin1** and **Quin2** were prepared using the literature procedures.^{46, 53}

All NMR spectra were recorded in the Max T. Rogers NMR Facility at Michigan State University using an Agilent DDR2 500 MHz NMR spectrometer equipped with a 5 mm PFG OneProbe operating at 500 MHz (^1H), 126 MHz (^{13}C), and 460 MHz (^{19}F).

All crystallographic data were collected at the Michigan State University Center for X-ray Crystallography. Single crystal diffraction data were collected from Rigaku Synergy S dual

source single crystal diffractometer using CuK α . Single crystals were mounted on glass fiber loops using N-paratone oil. Data collection was done at 173 K under a liquid nitrogen cold stream. The structures were solved with the ShelXT solution program using intrinsic phasing and refined with the XL refinement package using least squares minimization in Olex 2.

Synthesis of (η^6 (C6)-3-cyclohexyl-2,5,7-trimethylquinoline)(η^5 -cyclopentadienyl)ruthenium(II) hexafluorophosphate (1**):** This procedure was adapted from a literature synthesis.³⁰ In a glove box, tris(acetonitrile)(η^5 -cyclopentadienyl)ruthenium(II) hexafluorophosphate (43.4 mg, 0.1 mmol, 1.0 equiv) was dissolved in 2 mL of dry CH₂Cl₂ in a 20 mL glass vial. In a separate 20 mL vial, 3-cyclohexyl-2,5,7-trimethylquinoline (25.3 mg, 0.1 mmol, 1.0 equiv) was dissolved in 2 mL of CH₂Cl₂. The quinoline solution was added dropwise to the stirring solution of the acetonitrile complex to form a clear, yellow solution that was stirred for 1 h after addition. The solution was then layered with approximately 4 mL of OEt₂ and put in a freezer at -35 °C overnight. The next morning, off white crystals and powder (29.0 mg, 50%) were collected of **1**. M.p.: 226-227 °C. ¹H NMR (CDCl₃, 500 MHz, 21 °C): δ 7.96 (s, 1H), 6.85 (s, 1H), 6.43 (s, 1H), 4.92 (s, 5H), 2.83 (s, 3H), 2.71 (s, 3H), 2.48 (s, 3H), 2.03-1.77 (m, 5H), 1.53-1.43 (m, 5H). ¹³C{¹H} NMR (CDCl₃, 126 MHz, 21 °C): δ 169.92, 145.24, 130.08, 111.10, 102.45, 97.27, 92.09, 90.03, 84.41, 80.61, 40.72, 33.31, 33.16, 26.89, 26.85, 25.78, 24.24, 20.48, 18.00. ¹⁹F NMR (CDCl₃, 470 MHz, 21 °C): -71.52 (d, *J* = 713.3 Hz). Elemental analysis (with one equivalent dichloromethane in the lattice): calc'd for C₂₄H₃₀NF₆Cl₂PRu: C, 44.39; H, 4.66; N, 2.16. Found: C, 44.01; H, 4.68; N, 2.19. HRMS: QTOF EI (positive ion) calc'd for C₂₃H₂₈NRu: 420.1271; found: 420.1276.

Synthesis of (η^6 (C6)-3-(cyclohex-1-en-1-yl)-2-methylquinoline)(η^5 -cyclopentadienyl)ruthenium(II) hexafluorophosphate (2**):** In a glove box, tris(acetonitrile)(η^5 -cyclopentadienyl)ruthenium(II) hexafluorophosphate (20 mg, 1.0 equiv) was dissolved in 2 mL of dry dichloromethane in a 20 mL glass vial. In a separate 20 mL vial, 3-(cyclohex-1-en-1-yl)-2-methylquinoline (10.3 mg, 1.0 equiv) was dissolved in 2 mL of dichloromethane. The quinoline solution was added dropwise to the stirring solution of the acetonitrile complex to form a clear, yellow solution that was allowed to stir for 1 h. The solution was then layered with approximately 4 mL of diethyl ether and put in a freezer at -35 °C overnight. The next morning, off white crystals and powder (19.0 mg, 77%) were collected of **2**. M.p.: 185-187 °C. ¹H NMR (CDCl₃, 500 MHz, 21 °C): δ 7.84 (s, 1H), 7.12-7.04 (m, 1H), 7.04-6.95 (m, 1H), 6.38-6.28 (m, 2H), 5.75 (s, 1H), 5.08 (s, 5H), 2.65 (s, 3H), 2.27-2.18 (m, 4H), 1.84-1.70 (m, 4H). ¹³C{¹H} NMR (CDCl₃, 126 MHz, 21 °C): δ 170.30, 143.28, 136.04, 135.11, 130.37, 112.41, 92.79, 86.68, 86.15, 84.09, 84.02, 80.31, 29.62, 25.47, 25.18, 22.70, 21.71. ¹⁹F NMR (CDCl₃, 470 MHz, 21 °C): -72.50 (d, *J* = 712.2 Hz). HRMS: QTOF EI (positive ion) calc'd for C₂₁H₂₂NRu: 390.0801; found: 390.0802.

Synthesis of tris(dimethyl sulfoxide)(η^5 -cyclopentadienyl)ruthenium(II) hexafluorophosphate: A 20 mL glass vial was loaded with tris(acetonitrile)(η^5 -cyclopentadienyl)ruthenium(II) hexafluorophosphate (20 mg,

1.0 equiv) and a stir bar. To the solid, DMSO (84 mL, 12 equiv) was added, followed by 1 mL of H₂O. The reaction was kept stirring under vacuum at 60 °C for 12 h. The product was collected as an off white solid (50 mg, 93%). ¹H NMR (DMSO-d₆, 500 MHz, 25 °C): δ 5.47 (s, 5H), 3.50 (s, 18H). ¹³C{¹H} NMR (DMSO-d₆, 126 MHz, 25 °C): δ 85.74, 52.45. ¹⁹F NMR (DMSO-d₆, 470 MHz, 25 °C): δ -70.12 (d, *J* = 711.5 Hz). HRMS: QTOF EI (positive ion) calc'd for C₁₁H₂₃O₃S₃Ru: 400.9854; found: 400.9855.

Measurement of the kinetics of quinoline replacement by acetonitrile-d₃. In an inert atmosphere glove box, a 20 mL glass vial was loaded **1** (6.0 mg, 10.3 μ mol), ferrocene (as a reference, 2.0 mg, 10.75 μ mol), and acetonitrile-d₃ (600 μ L). The solution was mixed by drawing in and out of a pipet until homogeneous. The reaction was transferred into an NMR tube, which was carefully capped and sealed with electrical tape. Then, the NMR tube was removed from the glovebox and placed in room temperature a silicon oil bath. Periodically, an NMR tube was removed from the oil bath, and a ¹H NMR spectrum was measured. The relative concentration of **1** vs ferrocene was monitored as a function of time. The fits of the exponential decay of **1** were done using the scientific program KaleidaGraph v5.0.1. The expression used to fit the data was $Y_t = Y_\infty + (Y_0 - Y_\infty)e^{-k_{obs}t}$, where *Y* = concentration at time *t* (*Y_t*), infinity (*Y_∞*), or at the start of the reaction (*Y₀*).⁶⁰ An example of a plot of concentration vs time and its fit is shown in Fig. 3. Other experiments involving replacement of quinoline by solvent were done similarly. The plots and fits for the other trials, along with tabulated data, can be found in the SI.

Procedure for the 20S Proteasome Inhibition Activity Assay: The activity assay was conducted in a 100 μ L reaction volume in a black, clear-bottom 96-well plate. Purified human 20S proteasome (1 nM) and stock solutions of the test compound were added to final concentrations ranging from 1.25-80 μ M in assay buffer (50 mM Tris-HCl buffer, 0.03% SDS, pH 7.5), and the plate was incubated at 37 °C for 15 min. The fluorogenic substrates (Suc-LLVY-AMC, Boc-LRR-AMC, and Z-LLE-AMC) were added to a final concentration of 50 μ M for Suc-LLVY-AMC and Z-LLE-AMC, and a final concentration of 100 μ M for Boc-LRR-AMC. Fluorescence was measured at 37 °C on a SpectraMax M5e spectrometer taking kinetic readings every 1 min for 30 min (380/460 nm).

Cell viability assay. MC/CAR cells (5,000/well) were seeded in a white, opaque 96-well plate in 100 μ L of Iscove's Modified Dulbecco's Medium (IMDM) supplemented with 20% FBS and 1% penicillin/streptomycin. RPMI 8226 cells (25,000/well) were seeded in a white, opaque 96-well plate in 100 μ L of RPMI-1640 Medium supplemented with 10% FBS and 1% penicillin/streptomycin. Drug stock solutions were made in 100% DMSO-d₆ (Quin1 and Quin2) or 9:1 water/DMSO-d₆ (complexes **1** and **2**). The cells were then treated with the test compound at concentrations ranging from 1.25-40 μ M (0.5% DMSO-d₆ final concentration) for 72 hours at 37 °C and 5% CO₂. For samples in 100% DMSO-d₆, a total volume of 0.5 μ L drug stock was added; for samples in 9:1 water/DMSO-d₆, a total volume of 5 μ L drug stock was added. Cells were equilibrated to room temperature and CellTiter-Glo (Promega) solution (100

μL) was added and incubated with shaking for 2 minutes at room temperature. Assay plate was then allowed to equilibrate for 10 more minutes at room temperature and luminescence readings were taken on a SpectraMax M5e. Statistical analyses were performed with GraphPad Prism 8.1; Brown-Forsythe and Welch ANOVA with a post hoc Dunnett's T3 test was used for multiple comparisons of group means ($*p \leq 0.05$; $**p \leq 0.01$).

Cellular proteasome activity assay. RPMI 8226 cells (10,000/well) were seeded in a white, clear-bottom 96-well plate in 100 μL of RPMI-1640 medium supplemented with 10% FBS and 1% penicillin/streptomycin. The cells were then treated with DMSO, 10 μM test compound, or 50 nM BTZ (0.5% final DMSO concentration) for 4 h at 37 $^{\circ}\text{C}$ and 5% CO_2 . Cells were equilibrated to room temperature and Proteasome-Glo (CT-L site; Promega) solution (100 μL) was added and incubated with shaking for 12 min at room temperature. To an identical plate, CellTiter-Glo (Promega) solution (100 μL) was added and incubated with shaking for 2 min at room temperature. Assay plate was then allowed to equilibrate for 10 more min at room temperature. Luminescence readings were taken on a SpectraMax M5e. Statistical analyses were performed with GraphPad Prism 8.1; One-way ANOVA with a post hoc Sidak test was used for multiple comparisons of group means (ns = not significant; $*p \leq 0.05$; $**p \leq 0.01$; $***p \leq 0.001$; $****p \leq 0.0001$).

Cited References

1. B. Rosenberg, L. Vancamp and T. Krigas, *Nature*, 1965, **205**, 698.
2. B. Rosenberg, E. Renshaw, L. Vancamp, J. Hartwick and J. Drobnik, *J. Bacteriol.*, 1967, **93**, 716.
3. B. Rosenberg, L. Vancamp, J. E. Trosko and V. H. Mansour, *Nature*, 1969, **222**, 385.
4. T. C. Johnstone, K. Suntharalingam and S. J. Lippard, *Chem. Rev.*, 2016, **116**, 3436-3486.
5. E. S. Antonarakis and A. Emadi, *Cancer Chemother. Pharma.*, 2010, **66**, 1-9.
6. P. Kumar, I. Mondal, R. Kulshreshtha and A. K. Patra, *Dalton Trans.*, 2020, **49**, 13294-13310.
7. H. R. Wang, J. H. Wei, H. Jiang, Y. Zhang, C. N. Jiang and X. L. Ma, *Molecules*, 2021, **26**.
8. Y. C. Wang, J. H. Jin, L. W. Shu, T. Y. Li, S. M. Lu, M. K. M. Subarkhan, C. Chen and H. X. Wang, *Chem. Eur. J.*, 2020, **26**, 15170-15182.
9. I. Yousuf and M. Bashir, *Appl. Organomet. Chem.*, 2021, **35**.
10. J. Haribabu, S. Srividya, R. Umaphathi, D. Gayathri, P. Venkatesu, N. Bhuvanesh and R. Karvembu, *Inorg. Chem. Commun.*, 2020, **119**.
11. E. Alessio and L. Messori, *Molecules*, 2019, **24**.
12. A. Casini, C. G. Hartinger, A. A. Nazarov and P. J. Dyson, in *Medicinal Organometallic Chemistry*, eds. G. Jaouen and N. Metzler-Nolte, 2010, vol. 32, pp. 57-80.
13. R. G. Kenny and C. J. Marmion, *Chem. Rev.*, 2019, **119**, 1058-1137.
14. S. Medici, M. Peana, V. M. Nurchi, J. I. Lachowicz, G. Crisponi and M. A. Zoroddu, *Coord. Chem. Rev.*, 2015, **284**, 329-350.
15. S. M. Meier-Menches, C. Gerner, W. Berger, C. G. Hartinger and B. K. Keppler, *Chem. Soc. Rev.*, 2018, **47**, 909-928.

Author Contributions

ZH carried out the syntheses, characterization, and reactivity studies of the ruthenium complexes. ASV carried out the biological studies on the compounds and controls. JJT and ALO conceived of the studies, supplied resources, and aided in data interpretation. ALO wrote the initial draft of the manuscript and all authors contributed to editing and finalizing the manuscript.

Conflicts of interest

There are no conflicts to declare.

Acknowledgements

The authors would like to thank the National Science Foundation for generous support of this research (to ALO: 1953254 and 1919565) and the National Institute of Aging (to JJT: 5R01AG066223) of the National Institutes of Health. In addition, the Petroleum Research Fund administered by the American Chemical Society provide support in the form of a grant to ALO, PRF 65702-ND3.

Notes and references

16. B. S. Murray, M. V. Babak, C. G. Hartinger and P. J. Dyson, *Coord. Chem. Rev.*, 2016, **306**, 86-114.
17. A. A. Nazarov, C. G. Hartinger and P. J. Dyson, *J. Organomet. Chem.*, 2014, **751**, 251-260.
18. M. Patra and G. Gasser, *Nature Reviews Chemistry*, 2017, **1**.
19. G. Jaouen and P. J. Dyson, in *Comprehensive Organometallic Chemistry*, Elsevier, Amsterdam, 2007, vol. 12, pp. 445-461.
20. V. Brabec and O. Novakova, *Drug Resis. Up.*, 2006, **9**, 111-122.
21. M. R. Gill, P. J. Jarman, S. Halder, M. G. Walker, H. K. Saeed, J. A. Thomas, C. Smythe, K. Ramadan and K. A. Vallis, *Chem. Sci.*, 2018, **9**, 841-849.
22. J. D. Hoeschele, J. Kasparkova, H. Kosthunova, O. Novakova, J. Pracharova, P. Pineau and V. Brabec, *J. Biol. Inorg. Chem.*, 2020, **25**, 913-924.
23. C. Streu, L. Feng, P. J. Carroll, J. Maksimoska, R. Marmorstein and E. Meggers, *Inorg. Chim. Acta*, 2011, **377**, 34-41.
24. L. Corte-Real, M. P. Robalo, F. Marques, G. Nogueira, F. Avecilla, T. J. L. Silva, F. C. Santos, A. I. Tomaz, M. H. Garcia and A. Valente, *J. Inorg. Biochem.*, 2015, **150**, 148-159.
25. M. H. Garcia, T. S. Morais, P. Florindo, M. F. M. Piedade, V. Moreno, C. Ciudad and V. Noe, *J. Inorg. Biochem.*, 2009, **103**, 354-361.
26. T. Moreira, R. Francisco, E. Comsa, S. Duban-Deweer, V. Labas, A. P. Teixeira-Gomes, L. Combes-Soia, F. Marques, A. Matos, A. Favrelle, C. Rousseau, P. Zinck, P. Falson, M. H. Garcia, A. Preto and A. Valente, *Eur. J. Med. Chem.*, 2019, **168**, 373-384.
27. G. Zhu, J. M. Tanski, D. G. Churchill, K. E. Janak and G. Parkin, *Journal of the American Chemical Society*, 2002, **124**, 13658-13659.

28. R. H. Fish, R. H. Fong, A. Tran and E. Baralt, *Organometallics*, 1991, **10**, 1209-1212.
29. R. H. Fish, H. S. Kim and R. H. Fong, *Organometallics*, 1989, **8**, 1375-1377.
30. R. H. Fish, H. S. Kim and R. H. Fong, *Organometallics*, 1991, **10**, 770-777.
31. R. M. Fairchild and K. T. Holman, *Organometallics*, 2007, **26**, 4086-4086.
32. R. M. Fairchild and K. T. Holman, *Organometallics*, 2007, **26**, 3049-3053.
33. W. H. Ang, A. De Luca, C. Chapuis-Bernasconi, L. Juillerat-Jeanneret, M. Lo Bello and P. J. Dyson, *Chemmedchem*, 2007, **2**, 1799-1806.
34. N. Busto, J. Valladolid, C. Aliende, F. A. Jalon, B. R. Manzano, A. M. Rodriguez, J. F. Gaspar, C. Martins, T. Biver, G. Espino, J. M. Leal and B. Garcia, *Chem. Asian J.*, 2012, **7**, 788-801.
35. C. M. Clavel, E. Paunescu, P. Nowak-Sliwinska, A. W. Griffioen, R. Scopelliti and P. J. Dyson, *J. Med. Chem.*, 2015, **58**, 3356-3365.
36. P. R. Florindo, D. M. Pereira, P. M. Borralho, M. F. M. Piedade, M. C. Oliveira, A. M. Dias, C. M. P. Rodrigues and A. C. Fernandes, *New J. Chem.*, 2019, **43**, 1195-1201.
37. P. R. Florindo, D. M. Pereira, P. M. Borralho, C. M. P. Rodrigues, M. F. M. Piedade and A. C. Fernandes, *J. Med. Chem.*, 2015, **58**, 4339-4347.
38. B. T. Loughrey, B. V. Cuning, P. C. Healy, C. L. Brown, P. G. Parsons and M. L. Williams, *Chem. Asian J.*, 2012, **7**, 112-121.
39. B. T. Loughrey, M. L. Williams, P. C. Healy, A. Innocenti, D. Vullo, C. T. Supuran, P. G. Parsons and S. A. Poulsen, *J. Biol. Inorg. Chem.*, 2009, **14**, 935-945.
40. M. Melchart, A. Habtemariam, O. Novakova, S. A. Moggach, F. P. A. Fabbiani, S. Parsons, V. Brabec and P. J. Sadler, *Inorg. Chem.*, 2007, **46**, 8950-8962.
41. L. Ronconi and P. J. Sadler, *Coord. Chem. Rev.*, 2007, **251**, 1633-1648.
42. A. R. Simovic, R. Masnikosa, I. Bratsos and E. Alessio, *Coord. Chem. Rev.*, 2019, **398**.
43. F. Wang, H. M. Chen, S. Parsons, I. D. H. Oswald, J. E. Davidson and P. J. Sadler, *Chem. Eur. J.*, 2003, **9**, 5810-5820.
44. F. Y. Wang, A. Habtemariam, E. P. L. van der Geer, R. Fernandez, M. Melchart, R. J. Deeth, R. Aird, S. Guichard, F. P. A. Fabbiani, P. Lozano-Casal, I. D. H. Oswald, D. I. Jodrell, S. Parsons and P. J. Sadler, *Proc. Nat. Acad. Sci.*, 2005, **102**, 18269-18274.
45. Y. K. Yan, M. Melchart, A. Habtemariam, A. F. A. Peacock and P. J. Sadler, *J. Biol. Inorg. Chem.*, 2006, **11**, 483-488.
46. T. J. McDaniel, T. A. Lansdell, A. A. Dissanayake, L. M. Azevedo, J. Claes, A. L. Odom and J. J. Tepe, *Biorg. Med. Chem.*, 2016, **24**, 2441-2450.
47. L. D. Fricker, in *Annual Review of Pharmacology and Toxicology, Vol 60*, ed. P. A. Insel, 2020, vol. 60, pp. 457-476.
48. E. E. Manasanch and R. Z. Orłowski, *Nature Reviews Clinical Oncology*, 2017, **14**, 417-433.
49. L. M. Azevedo, T. A. Lansdell, J. R. Ludwig, R. A. Mosey, D. K. Woloch, D. P. Cogan, G. P. Patten, M. R. Kuszpit, J. S. Fisk and J. J. Tepe, *J. Med. Chem.*, 2013, **56**, 5974-5978.
50. P. Beck, T. A. Lansdell, N. M. Hewlett, J. J. Tepe and M. Groll, *Angew. Chem. Int. Ed.*, 2015, **54**, 2830-2833.
51. M. B. Giletto, P. A. Osmulski, C. L. Jones, M. E. Gaczynska and J. J. Tepe, *Org. Biomol. Chem.*, 2019, **17**, 2734-2746.
52. T. A. Lansdell, M. A. Hurchla, J. Y. Xiang, S. Hovde, K. N. Weilbaecher, R. W. Henry and J. J. Tepe, *ACS Chem Biol*, 2013, **8**, 578-587.
53. S. Majumder, K. R. Gipson and A. L. Odom, *Org. Lett.*, 2009, **11**, 4720-4723.
54. A. L. Odom and T. J. McDaniel, *Acc. Chem. Res.*, 2015, **48**, 2822-2833.
55. G. Golbaghi and A. Castonguay, *Molecules*, 2020, **25**, 265.
56. E. Konac, N. Varol, I. Kiliccioglu and C. Y. Bilen, *Oncol. Lett.*, 2015, **10**, 560-564.
57. R. Jan and G. E. S. Chaudhry, *Adv. Pharm. Bull.*, 2019, **9**, 205-218.
58. J. E. Davies and A. D. Bond, *Acta Crystallogr Sect E: Struct Rep Online*, 2001, **57**, o947-o949.
59. A. M. McNair and K. R. Mann, *Inorg. Chem.*, 1986, **25**, 2519-2527.
60. J. H. Espenson, *Chemical kinetics and reaction mechanisms*, McGraw Hill, New York, 2nd Edition edn., 2002.
61. D. P. Shoemaker, C. W. Garland and J. W. Nibler, *Experiments in physical chemistry*, McGraw-Hill, New York, 5th edn., 1989.
62. S. P. Nolan, K. L. Martin, E. D. Stevens and P. J. Fagan, *Organometallics*, 1992, **11**, 3947-3953.
63. N. V. Shvydkiy and D. S. Perekalin, *Coord. Chem. Rev.*, 2020, **411**.
64. M. E. Rerek, L. N. Ji and F. Basolo, *J. Chem. Soc., Chem. Commun.*, 1983, DOI: 10.1039/c39830001208, 1208-1209.
65. L. N. Ji, M. E. Rerek and F. Basolo, *Organometallics*, 1984, **3**, 740-745.
66. T. A. Thibaudeau and D. M. Smith, *Pharma. Rev.*, 2019, **71**, 170-197.
67. M. R. Eisele, R. G. Reed, T. Rudack, A. Schweitzer, F. Beck, I. Nagy, G. Pfeifer, J. M. Plitzko, W. Baumeister, R. J. Tomko and E. Sakata, *Cell Reports*, 2018, **24**, 1301.
68. D. Finley, X. Chen and K. J. Walters, *Trends Biochem. Sci*, 2016, **41**, 77-93.
69. G. W. Gokel, R. P. Widera and W. P. Weber, *Organic Syntheses*, 1976, **55**, 96.
70. Y. H. Shi, C. Hall, J. T. Ciszewski, C. S. Cao and A. L. Odom, *Chem. Commun.*, 2003, DOI: 10.1039/b212423h, 586-587.
71. T. P. Gill and K. R. Mann, *Organometallics*, 1982, **1**, 485-488.